Report

Current Biology

Correlation between ranges of leg walking angles and passive rest angles among leg types in stick insects

Highlights

- Walk horizontal body-to-leg angles differ by stick insect leg type
- Return angles after manual deflection of denervated legs also differ by leg type
- Walking and return body-to-leg angle ranges correlate in each leg type
- Example of evolution altering passive properties as behavior changes

Authors

Christoph Guschlbauer, Scott L. Hooper, Charalampos Mantziaris, Anna Schwarz, Nicholas S. Szczecinski, Ansgar Büschges

Correspondence

hooper@ohio.edu

In brief

The walk horizontal body-to-leg angles are more posterior in more posterior stick insect legs. In small limbs, passive forces play a large role in leg movement. Therefore, Guschlbauer et al. measured the return body-to-leg angles after the deflection of denervated legs. The walking and return angle ranges correlate, matching the passive properties of each leg to the leg's behavior.

Guschlbauer et al., 2022, Current Biology *32*, 2334–2340
May 23, 2022
https://doi.org/10.1016/j.cub.2022.04.013

CellPress

CellPress

Current Biology

Report

Correlation between ranges of leg walking angles and passive rest angles among leg types in stick insects

Christoph Guschlbauer,[1,4] Scott L. Hooper,[2,4,5,*] Charalampos Mantziaris,[1] Anna Schwarz,[1] Nicholas S. Szczecinski,[3] and Ansgar Büschges[1]

[1]Department of Biology, Institute of Zoology, University of Cologne, 50674 Cologne, Germany
[2]Department of Biological Sciences, Ohio University, Athens, OH 45701, USA
[3]Benjamin M. Statler College of Engineering and Mineral Resources, West Virginia University, Morgantown, WV 26506, USA
[4]These authors contributed equally
[5]Lead contact
*Correspondence: hooper@ohio.edu
https://doi.org/10.1016/j.cub.2022.04.013

SUMMARY

Because of scaling issues, passive muscle and joint forces become increasingly important as limb size decreases.[1–3] In some small limbs, passive forces can drive swing in locomotion,[4,5] and antagonist passive torques help control limb swing velocity.[6] In stance, minimizing antagonist muscle and joint passive forces could save energy. These considerations predict that, for small limbs, evolution would result in the angle range over which passive forces are too small to cause limb movement (called "resting-state range" in prior insect work[4] and "area of neutral equilibrium" in physics and engineering) correlating with the limb's typical working range, usually that in locomotion. We measured the most protracted and retracted thorax-femur (ThF) angles of the pro- (front), meso- (middle), and metathoracic (hind) leg during stick insect (*Carausius morosus*) walks. This ThF working range differed in the three leg types, being more posterior in more posterior legs. In other experiments, we manually protracted or retracted the denervated front, middle, and hind legs. Upon release, passive forces moved the leg in the opposite direction (retraction or protraction) until it reached the most protracted or most retracted edge of the ThF resting-state range. The ThF resting-state angle ranges correlated with the leg-type working range, being more posterior in more posterior legs. The most protracted ThF walking angles were more retracted than the post-protraction ThF angles, and the most retracted ThF walking angles were similar to the post-retraction ThF angles. These correlations of ThF working- and resting-state ranges could simplify motor control and save energy. These data also provide an example of evolution altering behavior by changing passive muscle and joint properties.[7]

RESULTS

Inactive muscles stretched beyond their rest length generate stretch-opposing passive forces. For joints with opposing muscles, joint rotation lengthens one (increasing its passive force on the limb) and shortens the other (decreasing its passive force on the limb). On release, the joint consequently rotates toward the angle at which the two muscle's passive forces counterbalance each other. Similar considerations apply to joint elastic tissues. When combined with joint friction (see discussion), these properties result in joints having a resting-state range within which they do not move or move only slightly when rotated to different angles within it and to the edges of which they return when rotated outside it.[4] Passive forces scale as limb size squared. Limb mass, which determines the importance of gravitational forces and limb inertia, scales as limb size cubed. Although there are exceptions,[8] passive forces are therefore typically most important in small limbs.[1–3]

Passive forces are important in small limb movements in invertebrates[1,2,4–6,9–15] and vertebrates[16–21] and have been applied to invertebrate[3,22–30] and vertebrate[3,31–35] motor system simulations and robot designs. These observations suggest that in small limbs, evolution should have resulted in joint resting-state range and typical working range being correlated.[7] Stick insect pro- (front), meso- (middle), and metathoracic (hind) legs are an excellent preparation in which to test this hypothesis. First, testing it requires limb types with different working ranges. Stick insect front, middle, and hind leg tarsus positions in stance are progressively more retracted.[36] The leg types have thus evolved into behaviorally different entities. Second, the techniques to examine passive properties are well developed in stick insects.[1,2,4,6,37,38]

The most proximal segments of stick insect legs are the coxa and fused trochanterofemur. The thorax-coxa (ThC) joint primarily produces protraction-retraction and pronation-supination.[10,39] The coxa-trochanterofemur (C-TF) joint is a hinge that rotates in the plane determined by ThC protraction

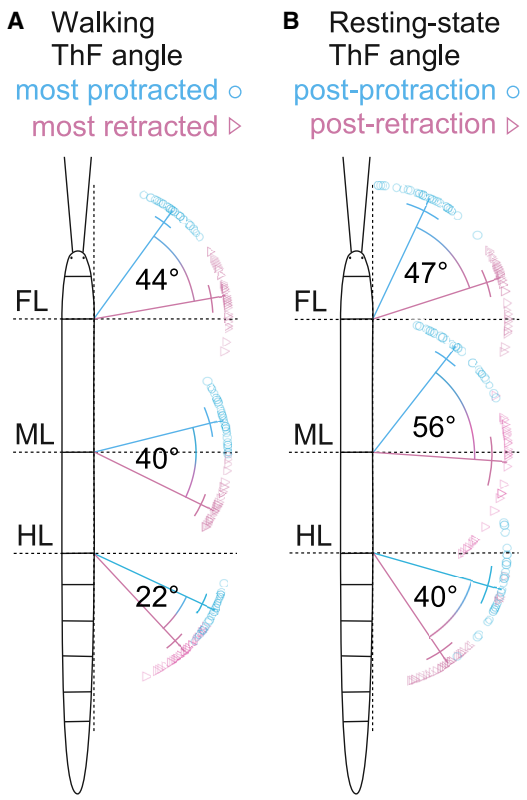

Figure 1. Each leg type's most protracted and most retracted ThF walking angles, and post-protraction and post-retraction angles, differed

Stick insect schematic, dorsal view and anterior up. Right leg ThF angles are shown. The horizontal and vertical dashed lines are 90° and 0°/180° ThF angles, respectively. Circles and triangles are data points. Overlying points have a denser color. The matched color lines are medians and median absolute deviations. Blue to magenta curved lines and the numbers are the median ThF ranges. (A) Front, middle, and hind leg (FL, ML, and HL) most protracted (blue) and most retracted (magenta) ThF walking angles. (B) Post-protraction (blue) and post-retraction (magenta) ThF resting-state angles. The blue and magenta data significantly differed in all cases (Table 1). Animal and trial numbers in the text.

and pronation.[10,39] Here, we use a combined metric (thorax-femur [ThF]), the angle between the longitudinal body axis and trochanterofemur in images obtained with a single camera located above the animal. In these two-dimensional projections of the three-dimensional situation, single ThF angles can arise from multiple ThC pronations and ThC and C-TF angles. Unique ThC and C-TF angles and pronations can therefore not be extracted from our data. However, a very prominent characteristic of stick insect walking is, by whatever combination of changes in individual leg joints, large trochanterofemur protraction and retraction. ThF angle is a simple measure of these movements.

Inter-animal variability[6,37,38,40–43] poses a potential difficulty in this work, e.g., animals whose front legs have particularly protracted ThF walking angle ranges might have particularly protracted ThF resting-state ranges. Having these individual animal correlations in the data can result in two possible sources of correlation, intra-animal correlation and across-population, presumably evolutionary, correlation. The most robust method to examine only across-population variation is to gather the behavioral and passive data from different animals. The two datasets are then independent and exclude any intra-animal correlation. Consistent with these considerations, walking and hold-and-release data were obtained from different animals and statistical comparisons made on across-animal pooled data. Some of the data were not normally distributed. Therefore, we used non-parametric statistical tests for all data comparisons.

In each leg type, the most protracted and most retracted ThF walking angles formed two distinct sets, as did post-protraction and post-retraction ThF resting angles

Most protracted and most retracted ThF walking angles were measured in five sequential steps from eight animals (N = 8, n = 40) (Figure 1A). The front leg's most protracted angles (blue circles) ranged from 22° to 52° (median 36°, blue line) and the most retracted (magenta triangles) from 60° to 104° (median 80°, magenta line), for a median walking angle range of 44°. The middle leg's most protracted angles ranged from 58° to 91° (median 76°) and the most retracted from 91° to 124° (median 116°), for a walking angle range of 40°. The hind leg's most protracted angles ranged from 103° to 131° (median 115°) and the most retracted from 123° to 157° (median 137°), for a walking angle range of 22°. Each leg type's most protracted and most retracted walking angle ranges thus formed largely non-overlapping, significantly different (Table 1) sets.

Post-protraction and post-retraction ThF angles were measured from three alternating protractions and retractions in twelve animals (N = 12, n = 36) (Figure 1B). The front leg post-protraction angles (blue circles) ranged from 2° to 51° (median 25°, blue line) and the post-retraction (magenta triangles) from 59° to 104° (median 72°, magenta line), for a median resting-state angle range of 47°. The middle leg post-protraction angles ranged from 19° to 66° (median 38°) and the post-retraction from 65° to 139° (median 94°), for a resting-state angle range of 56°. The hind leg post-protraction angles ranged from 77° to 141° (median 106°) and the post-retraction from 100° to 164° (median 146°), for a resting-state angle range of 40°. Each leg type's post-protraction and post-retraction angles thus formed largely non-overlapping, significantly different (Table 1) sets.

Most protracted and most retracted ThF walking angles, and post-protraction and post-retraction ThF angles, differed across legs

Plotting the Figure 1 data by leg type shows that the most protracted (Figure 2Ai) and most retracted (Figure 2Aii) ThF walking angles and the post-protraction (Figure 2Bi) and post-retraction (Figure 2Bii) ThF passive return angles significantly differed (Table 1) in the three leg types, although the front and middle leg post-protraction and post-retraction resting-state angles showed considerable overlap.

In all legs, most protracted ThF walking angles were more retracted than post-protraction ThF angles, and most retracted ThF walking angles were similar to post-retraction ThF angles

Combining the front, middle, and hind (Figures 3A–3C, respectively) leg active and passive data showed that the most protracted ThF walking angles (blue circles, lines) were significantly more

Table 1. p values and significance levels of comparisons made in Figures 1, 2, and 3

Comparison	p value	Result
Figure 1		
FL most protracted ThF walking versus FL most retracted ThF walking	1.39×10^{-14}	***
ML most protracted ThF walking versus ML most retracted ThF walking	1.43×10^{-14}	***
HL most protracted ThF walking versus HL most retracted ThF walking	4.14×10^{-13}	***
FL post-protraction ThF versus FL post-retraction ThF	3.00×10^{-13}	***
ML post-protraction ThF versus ML post-retraction ThF	3.25×10^{-13}	***
HL post-protraction ThF versus HL post-retraction ThF	3.50×10^{-10}	***
Figure 2		
FL most protracted ThF walking versus ML most protracted ThF walking	1.38×10^{-14}	***
FL most protracted ThF walking versus HL most protracted ThF walking	1.37×10^{-14}	***
ML most protracted ThF walking versus HL most protracted ThF walking	1.38×10^{-14}	***
FL most retracted ThF walking versus ML most retracted ThF walking	4.09×10^{-14}	***
FL most retracted ThF walking versus HL most retracted ThF walking	1.40×10^{-14}	***
ML most retracted ThF walking versus HL most retracted ThF walking	1.80×10^{-14}	***
FL post-protraction ThF versus ML post-protraction ThF	3.21×10^{-5}	***
FL post-protraction ThF versus HL post-protraction ThF	3.00×10^{-13}	***
ML post-protraction ThF versus HL post-protraction ThF	2.99×10^{-13}	***
FL post-retraction ThF versus ML post-retraction ThF	8.73×10^{-7}	***
FL post-retraction ThF versus HL post-retraction ThF	3.56×10^{-13}	***
ML post-retraction ThF versus HL post-retraction ThF	1.08×10^{-10}	***
Figure 3		
FL most protracted ThF walking versus FL post-protraction ThF	5.17×10^{-7}	***
ML most protracted ThF walking versus ML post-protraction ThF	1.72×10^{-13}	***
HL most protracted ThF walking versus HL post-protraction ThF	0.000257	**
FL most retracted ThF walking versus FL post-retraction ThF	0.288	n.s.
ML most retracted ThF walking versus ML post-retraction ThF	0.013	n.s.
HL most retracted ThF walking versus HL post-retraction ThF	0.00104	**

All two-sided Mann-Whitney U tests. Nominal α-level 0.05. Each condition used four times, giving Bonferroni-corrected significance values: n.s., $p > 0.0125$; *$p \leq 0.0125$; **$p \leq 0.0025$; ***$p \leq 0.00025$.

retracted than post-protraction ThF angles (magenta triangles, lines) in all legs (Table 1). Front and hind leg active and passive medians were nonetheless similar. For the middle leg, the medians differed substantially. The front and middle leg's most retracted ThF walking angles (black squares, lines) and post-retraction ThF angles (orange stars, lines) did not significantly differ. The hind leg's most retracted ThF walking angles were significantly more protracted than post-retraction ThF angles (Table 1), but again the medians were similar.

Active (the most protracted and most retracted ThF walking angles) and passive (post-protraction and post-retraction ThF angles) ThF angles were thus similar for the front and hind legs. The middle leg's most protracted ThF walking angles (blue, Figure 3B) were more retracted than post-protraction ThF angles (magenta, Figure 3B). The middle leg's most retracted ThF walking angles (black, Figure 3B) were primarily in the more retracted portion of the post-retraction ThF range (orange, Figure 3B).

DISCUSSION

Our data show that stick insect ThF resting-state and working ranges became progressively more retracted from front to hind leg and were similar for all leg types (Figure 3). These shifts result from combined anterior to posterior changes in joint, muscle, and nervous system properties. They are thus an excellent example of the Chiel and Beer[7] insight that the multiple systems that underlie movement production co-evolve as a holistic group.

Why are ThF passive rest angles a range?

For a two-muscle joint, passive muscle forces counterbalance each other at only one angle. Joint elastic tissues similarly presumably produce zero net force at only one angle. Post-protraction ThF angles (blue circles), however, are more protracted than post-retraction ThF angles (magenta triangles) (Figure 1B). Stick insect[1] and locust femur-tibia (FT) joints[4,9] also return to different angles after manual extension and flexion, which in locusts has been referred to as "history dependence."[9]

Passive rest angles presumably arise from an equilibrium being reached between (1) rotation-promoting forces arising from muscle and joint elastic tissue and (2) rotation-resisting friction or other forces. Assuming that rotation-resisting forces resemble Coulumb friction, the difference in post-protraction and post-retraction return angles can be understood by considering two

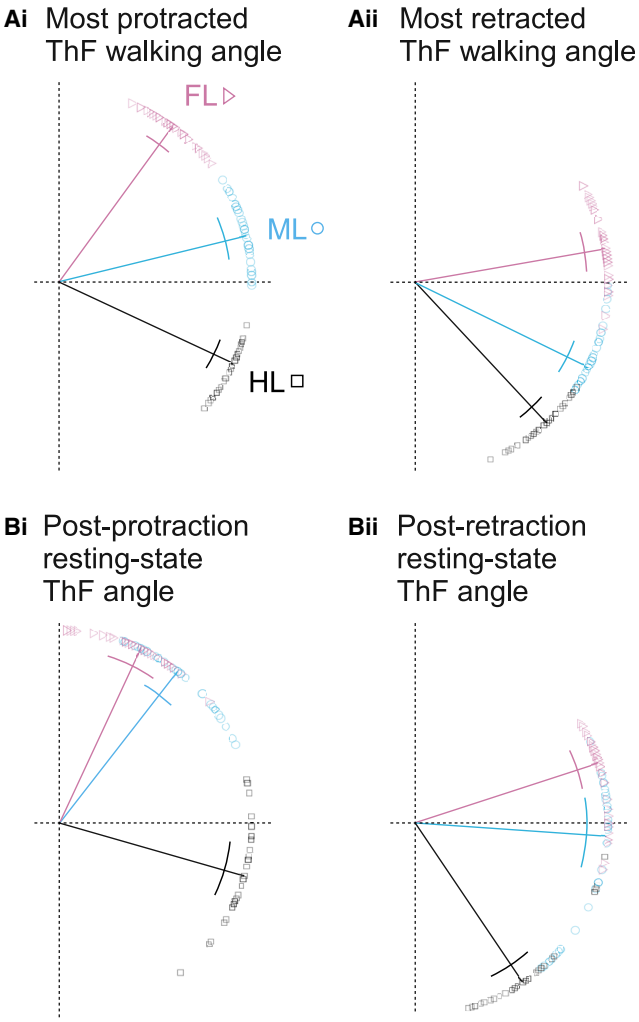

Figure 2. The most protracted and most retracted ThF walking angles and post-protraction and post-retraction ThF angles significantly differed across legs

Comparison of the data of the three leg types (FL, ML, and HL) in each experimental condition: walking ThF angle (Ai and Aii) and resting-state ThF angle (Bi and Bii). Same data and figure conventions as in Figure 1. Statistical tests are in Table 1.

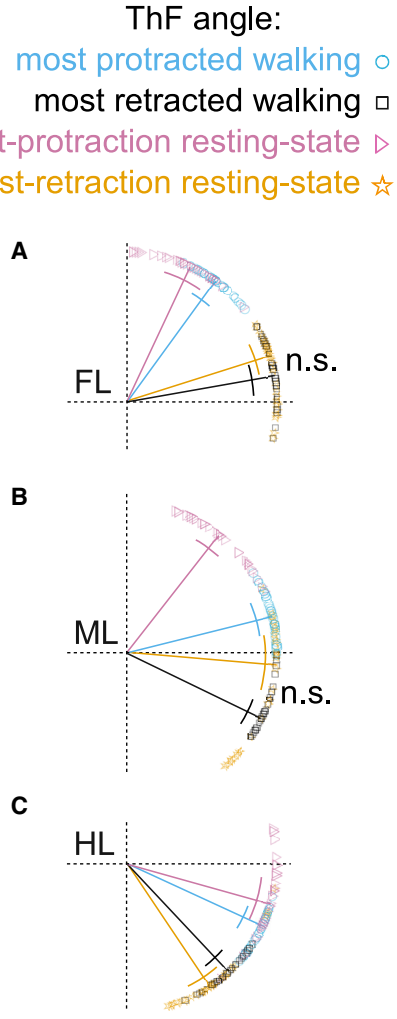

Figure 3. Comparison of most protracted and most retracted ThF walking angles and post-retraction and post-protraction ThF angles in all legs

The most protracted ThF walking angles were more retracted than post-protraction ThF angles in all legs. The most retracted ThF walking angles were more protracted than post-retraction ThF angles in the hind leg and the same in others. Same data and figure conventions as in Figure 1. The most protracted ThF walking angles (blue circles) were significantly more retracted than the post-protraction ThF angles (magenta triangles) for all legs (FL, A; ML, B; HL, C). FL and ML most retracted ThF walking angles (black squares) and post-retraction ThF angles (orange stars) were not significantly different. HL most retracted ThF walking angles were significantly more protracted than post-retraction ThF angles, but the difference was small. Statistical tests are in Table 1.

bricks initially set high (where the slope is large) on the two arms of a downward-sloping (concave, $y = x^2$) parabolic ramp. Initially, the gravitational force on each brick is greater than the friction between the brick and the ramp, and the bricks slide downhill. As the bricks do so, the ramp slope decreases. The bricks stop sliding not at the gravitational potential energy minimum (ramp bottom) but instead at the ramp locations where each arm's slope is too small to overcome the friction between the brick and the ramp. Post-protraction and post-retraction return angles presumably differ due to an analogous mechanism—even though at both the post-protraction and post-retraction return angles rotation-promoting passive forces are not yet zero, they have become too small to overcome rotation-resisting forces. Such an area of neutral equilibrium exists in the locust FT joint—imposed rotations within this "resting-state range" (nomenclature Ache and Matheson[4]) induce only small or no return movements.[4]

The resting-state range will depend on muscle passive FL curves, joint force-angle curves, joint friction-like forces, and (presumably because of the dynamic nature of passive forces[6]) joint rotation and muscle activation history.[9] Which property is most important varies across species. In crabs and cockroaches, muscle passive forces primarily determine passive joint angles.[44] In locust and false stick insect (*Pseudoproscopia*

scabra) hind leg FT joints, muscle forces primarily determine post-flexion returns, but joint forces determine post-extension returns.[4] In stick insect middle leg, joint forces primarily determine post-flexion returns, but muscle forces determine post-extension returns.[1,4] In false stick insect middle leg, muscle and joint forces underlie returns in both directions.[4]

Repeated cycles of motor-neuron-induced extensions followed by passive returns can shift return angles,[9] in the extreme by as much as 5°. Such shifts did not occur in our work, presumably because we examined alternating movements. In any case, the shifts observed in Ache and Matheson[9] were too small to affect the conclusions presented here.

Mechanisms underlying shifts in ThF passive resting-state ranges

Resting-state range became progressively more retracted in the front, middle, and hind legs. This shift is likely largely due to muscle anatomical differences.[45,46] The functionally most important protractor, the pleural protractor, attaches to a different site in the pro- than the meso- and metathorax and has a larger moment arm in the pro- and mesothorax. The sternal and pleural retractors become progressively stronger moving anterior to posterior. Additionally, in the metathorax, the tergal protractor is absent and the sternal adductor becomes a retractor. The protractor muscle complex thus becomes progressively weaker, and the retractor muscle complex becomes progressively stronger, moving from anterior to posterior.[45]

Another source of leg-to-leg differences could be different muscle passive resistances to stretch. The half-sarcomere spanning protein, titin, is primarily responsible for vertebrate skeletal muscle passive force.[47] Analogous giant muscle proteins exist in invertebrates.[48–50] Calcium, phosphorylation, and alternative splicing can alter titin stiffness.[51] In rabbits, muscles with different passive stiffnesses express different titin isoforms.[52] Whether such differences exist in stick insect leg muscles is unknown. Nonetheless, the anatomical differences described above, likely changes in joint anatomy, and possible giant muscle protein differences provide ample mechanisms to explain the different resting-state angle ranges present in different stick insect legs.

Functional advantages of correlating most protracted ThF walking angles and post-protraction ThF angles and most retracted ThF walking angles and post-retraction ThF angles

ThF resting-state ranges were large for all legs (Figure 1B). Stick insect middle,[1] locust hind,[4,9] and false stick insect middle and hind[4] leg FT joints also have wide resting-state ranges. In the stick insect, the ThF walking- and resting-state ranges were similar for the front and hind legs (Figure 3). This correlation is advantageous for energy utilization because it means that antagonist passive forces are small enough in walking that only a small percentage of agonist active force is needed to overcome them to move the leg. For the middle leg, the most protracted walking angles (blue circles) were substantially more retracted than those of the post-protraction edge of the resting-state range (magenta triangles). Thus, passive forces should again play a little role at the most protracted middle leg walking angles. The majority of the most retracted angles in walking (black squares), alternatively, lay in the most retracted third of the post-retraction ThF angle range (orange stars). Passive protraction forces may thus assist stance to swing transitions in some steps.

Stick insects perform a much wider range of leg movements than those present in walking (e.g., in climbing and searching). In these movements, the ThF angles may be outside the resting-state range and passive forces would thus contribute to leg movement. Passive forces might even be sufficient to produce movement without neural input, as occurs in other insects.[4,5,53] Thus, passive forces could simplify some of the mechanisms proposed to underlie leg movement.[54–56]

Do working and resting angle ranges correlate in general?

Demonstrating the correlation shown here requires finding joints or joint systems (presumably small) with different working angle ranges, measuring the resting-state ranges of the joint or system, and testing if these ranges correlate. We have not found work in which this comparison has been performed. We did find the following cases where this comparison could be made or where work from multiple sources suggests it may exist. (1) Ache and Matheson[4] showed that passive forces have varying importance in FT joint movement in different insects but did not measure working ranges.[4] Doing so would allow testing for correlations between resting-state and working angle ranges. (2) Data from toad muscles suggest that active and passive muscle properties are correlated.[57] Toads use their hindlimb plantaris muscle mainly to produce jumping force and their forelimb anconeus muscle to produce braking forces on landing. The two muscles work on different parts of the FL curve and have different passive stiffnesses.[57] (3) A meta-analysis of multiple vertebrate species showed a negative correlation between muscle stiffness and joint movement range, although this correlation was absent in the four anuran species investigated.[58] These examples suggest that invertebrate and vertebrate preparations are available in which the correlation tested here can be performed.

STAR★METHODS

Detailed methods are provided in the online version of this paper and include the following:

- KEY RESOURCES TABLE
- RESOURCE AVAILABILITY
  - Lead contact
  - Materials availability
  - Data and code availability
- EXPERIMENTAL MODEL AND SUBJECT DETAILS
- METHOD DETAILS
  - Post-deflection ThF passive return angles
  - Walking ThF angles
- QUANTIFICATION AND STATISTICAL ANALYSIS

ACKNOWLEDGMENTS

We thank Till Bockemühl for help with the statistical analyses, Robert Rockenfeller for helpful discussion on the manuscript, Manfred Nebcke for measuring the ThF angles, and Michael Dübbert from the Animal Physiology

Department's Electronics Workshop at the University of Cologne for technical support. This research was supported by the NSF NeuroNex grant #2015317 to N.S.S. and A.B. (DFG-grant Bu857/15-1) and the NSF CRCNS grant #2113028 to N.S.S. (in collaboration with A.B.).

AUTHOR CONTRIBUTIONS

Conceptualization, C.G., S.L.H., and N.S.S.; methodology, C.G. and S.L.H.; formal analysis, C.M., C.G., and S.L.H.; investigation, C.M., A.S., and S.L.H.; resources, A.B.; data curation, S.L.H. and C.M.; writing – original draft, C.G.; writing – review & editing, all authors; visualization, C.M. and S.L.H.; supervision, C.G. and S.L.H.; project administration, C.G., S.L.H., and A.B.; funding acquisition, A.B.

DECLARATION OF INTERESTS

The authors declare no competing interests.

Received: October 2, 2021
Revised: February 7, 2022
Accepted: April 6, 2022
Published: April 26, 2022

REFERENCES

1. Hooper, S.L., Guschlbauer, C., Blümel, M., Rosenbaum, P., Gruhn, M., Akay, T., and Büschges, A. (2009). Neural control of unloaded leg posture and of leg swing in stick insect, cockroach, and mouse differs from that in larger animals. J. Neurosci. *29*, 4109–4119.
2. Hooper, S.L. (2012). Body size and the neural control of movement. Curr. Biol. *22*, R318–R322.
3. Young, F.R., Chiel, H.J., Tresch, M.C., Heckman, C.J., Hunt, A.J., and Quinn, R.D. (2022). Analyzing modeled torque profiles to understand scale-dependent active muscle responses in the hip joint. Biomimetics (Basel) *7*, 17.
4. Ache, J.M., and Matheson, T. (2013). Passive joint forces are tuned to limb use in insects and drive movements without motor activity. Curr. Biol. *23*, 1418–1426.
5. Page, K.L., Zakotnik, J., Dürr, V., and Matheson, T. (2008). Motor control of aimed limb movements in an insect. J. Neurophysiol. *99*, 484–499.
6. von Twickel, A., Guschlbauer, C., Hooper, S.L., and Büschges, A. (2019). Swing velocity profiles of small limbs can arise from transient passive torques of the antagonist muscle alone. Curr. Biol. *29*, 1–12.e7.
7. Chiel, H.J., and Beer, R.D. (1997). The brain has a body: adaptive behavior emerges from interactions of nervous system, body and environment. Trends Neurosci. *20*, 553–557.
8. Whittington, B., Silder, A., Heiderscheit, B., and Thelen, D.G. (2008). The contribution of passive-elastic mechanisms to lower extremity joint kinetics during human walking. Gait Posture *27*, 628–634.
9. Ache, J.M., and Matheson, T. (2012). Passive resting state and history of antagonist muscle activity shape active extensions in an insect limb. J. Neurophysiol. *107*, 2756–2768.
10. Dallmann, C.J., Dürr, V., and Schmitz, J. (2016). Joint torques in a freely walking insect reveal distinct functions of leg joints in propulsion and posture control. Proc. Biol. Sci. *283*, 20151708.
11. Godlewska-Hammel, E., Büschges, A., and Gruhn, M. (2017). Fiber-type distribution in insect leg muscles parallels similarities and differences in the functional role of insect walking legs. J. Comp. Physiol. A Neuroethol. Sens. Neural Behav. Physiol. *203*, 773–790.
12. Rosenbaum, P., Wosnitza, A., Büschges, A., and Gruhn, M. (2010). Activity patterns and timing of muscle activity in the forward walking and backward walking stick insect *Carausius morosus*. J. Neurophysiol. *104*, 1681–1695.
13. Szczecinski, N.S., Bockemühl, T., Chockley, A.S., and Büschges, A. (2018). Static stability predicts the continuum of interleg coordination patterns in *Drosophila*. J. Exp. Biol. *221*, jeb189142.
14. Weihmann, T. (2020). Survey of biomechanical aspects of arthropod terrestrialisation – substrate bound legged locomotion. Arthropod Struct. Dev. *59*, 100983.
15. Zakotnik, J., Matheson, T., and Dürr, V. (2006). Co-contraction and passive forces facilitate load compensation of aimed limb movements. J. Neurosci. *26*, 4995–5007.
16. Biknevicius, A.R., Reilly, S.M., McElroy, E.J., and Bennett, M.B. (2013). Symmetrical gaits and center of mass mechanics in small-bodied, primitive mammals. Zoology (Jena) *116*, 67–74.
17. Biknevicius, A., Reilly, S., and Kljuno, E. (2016). Locomotion in small tetrapods: concepts and applications. In Understanding Mammalian Locomotion, J.E.A. Bertram, ed. (Wiley).
18. Gaveau, J., Berret, B., Demougeot, L., Fadiga, L., Pozzo, T., and Papaxanthis, C. (2014). Energy-related optimal control accounts for gravitational load: comparing shoulder, elbow, and wrist rotations. J. Neurophysiol. *111*, 4–16.
19. Peaden, A.W., and Charles, S.K. (2014). Dynamics of wrist and forearm rotations. J. Biomech. *47*, 2779–2785.
20. Mohamed Thangal, S.N.M., and Donelan, J.M. (2020). Scaling of inertial delays in terrestrial mammals. PLoS One *15*, e0217188.
21. Wu, M.M., Pai, D.K., Tresch, M.C., and Sandercock, T.G. (2012). Passive elastic properties of the rat ankle. J. Biomech. *45*, 1728–1732.
22. Ayali, A., Borgmann, A., Büschges, A., Couzin-Fuchs, E., Daun-Gruhn, S., and Holmes, P. (2015). The comparative investigation of the stick insect and cockroach models in the study of insect locomotion. Curr. Opin. Insect Sci. *12*, 1–10.
23. Goldsmith, C.A., Szczecinski, N.S., and Quinn, R.D. (2020). Neurodynamic modeling of the fruit fly *Drosophila melanogaster*. Bioinspir Biomim *15*, 065003.
24. Knops, S., Tóth, T.I., Guschlbauer, C., Gruhn, M., and Daun-Gruhn, S. (2013). A neuromechanical model for the neuronal basis of curve walking in the stick insect. J. Neurophysiol. *109*, 679–691.
25. Naris, M., Szczecinski, N.S., and Quinn, R.D. (2020). A neuromechanical model exploring the role of the common inhibitor motor neuron in insect locomotion. Biol. Cybern. *114*, 23–41.
26. Rubeo, S., Szczecinski, N., and Quinn, R. (2018). A synthetic nervous system controls a simulated cockroach. Appl. Sci. *8*, 6.
27. Tóth, T.I., Grabowska, M., Schmidt, J., Büschges, A., and Daun-Gruhn, S. (2013). A neuro-mechanical model explaining the physiological role of fast and slow muscle fibres at stop and start of stepping of an insect leg. PLoS One *8*, e78246.
28. Tóth, T.I., and Daun, S. (2017). Effects of functional decoupling of a leg in a model of stick insect walking incorporating three ipsilateral legs. Physiol. Rep. *5*, e13154.
29. Szczecinski, N.S., Goldsmith, C.A., Young, F.R., and Quinn, R.D. (2019). Tuning a robot servomotor to exhibit muscle-like dynamics. In Conference on Biomimetic and Biohybrid Systems. Living Machines 2019. Lecture Notes in Computer Science (Springer International Publishing), pp. 254–265.
30. von Twickel, A., Büschges, A., and Pasemann, F. (2011). Deriving neural network controllers from neuro-biological data: implementation of a single-leg stick insect controller. Biol. Cybern. *104*, 95–119.
31. Binder-Markey, B.I., and Murray, W.M. (2017). Incorporating the length-dependent passive-force generating muscle properties of the extrinsic finger muscles into a wrist and finger biomechanical musculoskeletal model. J. Biomech. *61*, 250–257.
32. Hunt, A.J., Szczecinski, N.S., Andrada, E., Fischer, M., and Quinn, R.D. (2015). Using animal data and neural dynamics to reverse engineer a neuromechanical rat model. In Conference on Biomimetic and Biohybrid Systems. Living Machines 2015. Lecture Notes in Computer Science, *9222*, S. Wilson, P. Verschure, A. Mura, and T. Prescott, eds. (Springer), pp. 211–222.

33. Hunt, A., Szczecinski, N., and Quinn, R. (2017). Development and training of a neural controller for hind leg walking in a dog robot. Front. Neurorobot. *11*, 18.

34. Jarc, A.M., Berniker, M., and Tresch, M.C. (2013). FES control of isometric forces in the rat hindlimb using many muscles. IEEE Trans. Biomed. Eng. *60*, 1422–1430.

35. Young, F., Hunt, A.J., and Quinn, R.D. (2018). A neuromechanical rat model with a complete set of hind limb muscles. In Conference on Biomimetic and Biohybrid Systems. Living Machines 2018. Lecture Notes in Computer Science, V. Vouloutsi, J. Halloy, A. Mura, M. Mangan, N. Lepora, T.J. Prescott, and P.F.M.J. Verschure, eds. (Springer), pp. 527–537, 10928.

36. Cruse, H. (1976). The function of the legs in the free walking stick insect, *Carausius morosus*. J. Comp. Physiol. *112*, 235–262.

37. Blümel, M., Hooper, S.L., Guschlbauer, C., White, W.E., and Büschges, A. (2012). Determining all parameters necessary to build hill-type muscle models from experiments on single muscles. Biol. Cybern. *106*, 543–558.

38. Guschlbauer, C., Scharstein, H., and Büschges, A. (2007). The extensor tibiae muscle of the stick insect: biomechanical properties of an insect walking leg muscle. J. Exp. Biol. *210*, 1092–1108.

39. Cruse, H., and Bartling, C. (1995). Movement of joint angles in the legs of a walking insect, *Carausius morosus*. J. Insect Physiol. *41*, 761–771.

40. Blümel, M., Guschlbauer, C., Daun-Gruhn, S., Hooper, S.L., and Büschges, A. (2012). Hill-type muscle model parameters determined from experiments on single muscles show large animal-to-animal variation. Biol. Cybern. *106*, 559–571.

41. Blümel, M., Guschlbauer, C., Hooper, S.L., and Büschges, A. (2012). Using individual-muscle specific instead of across-muscle mean data halves muscle simulation error. Biol. Cybern. *106*, 573–585.

42. Hooper, S.L., Guschlbauer, C., von Uckermann, G., and Büschges, A. (2006). Natural neural output that produces highly variable locomotory movements. J. Neurophysiol. *96*, 2072–2088.

43. Hooper, S.L., Guschlbauer, C., von Uckermann, G., and Büschges, A. (2007). Slow temporal filtering may largely explain the transformation of stick insect (*Carausius morosus*) extensor motor neuron activity into muscle movement. J. Neurophysiol. *98*, 1718–1732.

44. Yox, D.P., DiCaprio, R.A., and Fourtner, C.R. (1982). Resting tension and posture in arthropods. J. Exp. Biol. *96*, 421–425.

45. Marquardt, F. (1939). Beiträge zur Anatomie der Muskulatur und der peripheren Nerven von *Carausius* (*Dixippus) morosus*. Zool. Jahrb. Abt. Anat. Ont. Tiere *66*, 63–128.

46. Jeziorski, L. (1918). Der Thorax von Dixippus (*Carausius) morosus*. Z. Wiss. Zool. *117*, 727–815.

47. Brynnel, A., Hernandez, Y., Kiss, B., Lindqvist, J., Adler, M., Kolb, J., van der Pijl, R., Gohlke, J., Strom, J., Smith, J., et al. (2018). Downsizing the molecular spring of the giant protein titin reveals that skeletal muscle titin determines passive stiffness and drives longitudinal hypertrophy. eLife *7*, e40532.

48. Hooper, S.L., Hobbs, K.H., and Thuma, J.B. (2008). Invertebrate muscles: thin and thick filament structure; molecular basis of contraction and its regulation, catch and asynchronous muscle. Prog. Neurobiol. *86*, 72–127.

49. Hooper, S.L., and Thuma, J.B. (2005). Invertebrate muscles: muscle specific genes and proteins. Physiol. Rev. *85*, 1001–1060.

50. Thuma, J.B., and Hooper, S.L. (2010). Direct evidence that stomatogastric (*Panulirus interruptus*) muscle passive responses are not due to background actomyosin cross-bridges. J. Comp. Physiol. A *196*, 649–657.

51. Granzier, H.L., and Labeit, S. (2006). The giant muscle protein titin is an adjustable molecular spring. Exerc. Sport Sci. Rev. *34*, 50–53.

52. Horowits, R. (1992). Passive force generation and titin isoforms in mammalian skeletal muscle. Biophys. J. *61*, 392–398.

53. Berkowitz, A., and Laurent, G. (1996). Local control of leg movements and motor patterns during grooming in locusts. J. Neurosci. *16*, 8067–8078.

54. Bidaye, S.S., Bockemühl, T., and Büschges, A. (2018). Six-legged walking in insects: how CPGs, peripheral feedback, and descending signals generate coordinated and adaptive motor rhythms. J. Neurophysiol. *119*, 459–475.

55. Daun-Gruhn, S., and Büschges, A. (2011). From neuron to behavior: dynamic equation-based prediction of biological processes in motor control. Biol. Cybern. *105*, 71–88.

56. Schilling, M., and Cruse, H. (2020). Decentralized control of insect walking: a simple neural network explains a wide range of behavioral and neurophysiological results. PLoS Comput. Biol. *16*, e1007804.

57. Azizi, E. (2014). Locomotor function shapes the passive mechanical properties and operating lengths of muscle. Proc. Biol. Sci. *281*, 20132914.

58. Danos, D., and Azizi, E. (2015). Passive stiffness of hindlimb muscles in anurans with distinct locomotor specializations. Zoology *118*, 239–247.

59. Liessem, S., Ragionieri, L., Neupert, S., Büschges, A., and Predel, R. (2018). Transcriptomic and neuropeptidomic analysis of the stick insect, *Carausius morosus*. J. Proteome Res. *17*, 2192–2204.

60. Liessem, S., Kowatschew, D., Dippel, S., Blanke, A., Korsching, S., Guschlbauer, C., Hooper, S.L., Predel, R., and Büschges, A. (2021). Neuromodulation can be simple: myoinhibitory peptide, contained in dedicated regulatory pathways, is the only neurally-mediated peptide modulator of stick insect leg muscle. J. Neurosci. *41*, 2911–2929.

61. Campbell, K.S., and Moss, R.L. (2000). A thixotropic effect in contracting rabbit psoas muscle: prior movement reduces the initial tension response to stretch. J. Physiol. *525*, 531–548.

62. Lakie, M., and Campbell, K.S. (2019). Muscle thixotropy–where are we now? J. Appl. Physiol. *126* (1985), 1790–1799.

63. Wong, B. (2011). Color blindness. Nat. Methods *8*, 441.

STAR★METHODS

KEY RESOURCES TABLE

REAGENT or RESOURCE	SOURCE	IDENTIFIER
Deposited data		
ThF angle measurements and corresponding photos and movie stills	This paper; The Research Repository @ WVU	The Research Repository @ WVU: https://doi.org/10.33915/datasets.1
Experimental models: Organisms/strains		
Carausius morosus	Colony at University of Cologne	N/A

RESOURCE AVAILABILITY

Lead contact

Further information and requests for resources and reagents should be directed to and will be fulfilled by the lead contact, Scott L. Hooper (hooper@ohio.edu).

Materials availability

This study did not create any new reagents.

Data and code availability

- All ThF angle measurements and the corresponding photos and movie stills have been deposited as TXT and JPG files, respectively, at The Research Repository @ WVU and are publicly available as of the date of publication. The DOI is listed in the key resources table.
- This paper does not report original code.
- Any additional information required to reanalyze the data reported in this paper is available from the lead contact upon request.

EXPERIMENTAL MODEL AND SUBJECT DETAILS

Experiments were carried out on 20 sturdy adult female *Carausius morosus* from the Büschges lab colony at the Biocenter of the University of Cologne. Stick insects were held at a 12:12h light:dark cycle and fed with fresh blackberry leaves semi-weekly. Care was taken to select animals with a robust, hardened cuticle for the experiments examining passive return angles after deflection.

METHOD DETAILS

Post-deflection ThF passive return angles

Preparation

Experiments were done at room temperature (20-24°) under daylight conditions. Stick insects were glued using dental cement (ProTemp II, 3M Deutschland GmbH, Neuss, Germany) with the ventral side to a balsa wood rod mounted on a micromanipulator. The animal was placed on the rod such that the right front, middle, and hind leg coxae hung over the edge of the rod and the legs could move freely in all planes. The rod was placed in the holder such that the animal's body was horizontal both along the animal's length and width, i.e., at the position the body would have when upright. Left legs were amputated mid coxa. Right legs were deafferented and deefferented either from the dorsal (N=9) or ventral (N=3) side. Dorsal denervation was performed by making a small incision on the right dorsal side of the thorax close to the thorax-coxa (ThC) joint and cutting twice into the incision at each leg with micro scissors to transect all side nerves innervating leg muscles. Denervation success was verified by tickling the animal's abdomen: if the legs did not move in response, denervation was considered successful. Ventral denervation was achieved by cutting a small window in each thoracic segment and removing its ganglion, after which no test of denervation success was performed.

Denervated legs remained in the splayed posture typical of inactive innervated animals held horizontally upright without tarsus contact on a substrate. This result was expected, as the ThC joint primarily moves in the protraction/retraction plane[10,39] with ThC depression angle being the same in alive and dead animals[36] and often assumed to be a constant during walking.[10,36] Denervated legs assumed an angle in the protraction/retraction angle resting-state range, as expected from the data presented in the manuscript. The coxa-trochanterofemur joint assumed approximately its most allowed depressed angle (about 200°),[36] that is, with the long axes of the coxa and trochanterofemur being in an essentially straight line.

A possible concern in these experiments, as with the vast majority of muscle work, is that axons in the motor nerves innervating the muscles might release modulatory substances that alter passive muscle properties, and this release is altered when the nerves are cut. However, the complete neuropeptide complement of the stick insect has been recently described.[59] The only neurally-released peptide neuromodulator in the leg neuromuscular system does not affect extensor muscle passive properties.[60] The passive properties of other muscles were not checked in this work. It thus does not show that protractor and retractor muscle passive properties are not modulated by the peptide. It does show, however, that modulation of muscle passive properties by this peptide is not a general property of leg muscle.

Hold-and-release experiments

Our goal in these experiments was to measure ThF protraction/retraction resting-state angle ranges. ThF protraction/retraction changes were achieved by deflecting the entire leg horizontally anterior or posterior by manually moving the trochanterofemur perpendicular to the direction of gravity. The ThC joint both pronates/supinates and protracts/retracts.[10,39] No attempt was made to prevent pronation/supination.

Legs were protracted or retracted far from their resting-state angles, to the maximum the experimenter felt could be achieved without damaging the leg or joints. Except for front leg retraction, legs could be protracted to 0 to 10° and retracted to 170 to 180°. Front leg maximum retraction was photographed in most animals and ranged from 118 to 162° with a median of 152° (N=8, n=24). The leg was held in the maximally protracted or retracted position for 10 seconds to allow transient passive forces[6] of the stretched muscle (*retractor coxae* for protractions, *protractor coxae* for retractions) to decay. The leg was then released, upon which it moved in the direction opposite the deflection. ThF rotation was largely complete by 10 s (see also Ache and Matheson[4,9]), at which time a picture of the leg was taken with an Olympus E-330 camera mounted on a tripod. Lighting and focal plane could vary from picture to picture. Three protraction-retraction cycles, always beginning with protraction, were performed for each leg. Alternating cycles, as opposed to performing three protraction cycles and then three retraction cycles, were chosen because they are physiologically more relevant (in stick insect locomotion, the legs alternately protract and retract), several authors have shown that repeated of the same sort can cause changes in the dynamics of passive responses,[6,61,62] and Ache and Matheson[9] have shown that repeated movements of one sort (motor-neuron-induced extensions in their case) can induce increasing shifts in return angle. Hind legs were examined first. Each leg was amputated after examination and the adjacent rostral leg then examined.

A possible concern with this protocol was that the joint might become more compliant or otherwise change during the repeated protraction/retraction sequence, e.g., return to progressively smaller angles in protraction/retraction cycles 1, 2, and 3. However, a Kruskal-Wallis Rank Sum Test in Kaleidagraph (Synergy Software, Reading, PA, USA) showed no dependence on trial number for either post-protraction or post-retraction return angle for any leg.

ThF angle measurement

ThF angles in the pictures were measured as in the walking videos (see below), except that the thorax-trochanterofemur line was extended to the FT joint. Body orientation was identified, for each leg, by one line running along the longitudinal body axis at the position where the leg being examined left the thorax. The angle between these two lines (the ThF angle) was measured using a Canvas (Deneba, Miami, FL, USA) built-in tool that measures the angle between two lines. Measurement accuracy was estimated to be 1°, and the angles measured by the Canvas built-in tool were therefore rounded to 1°.

Walking ThF angles

Movies of walking animals

Walks were filmed from above using an AOS Technologies S-PRI color camera with 5.2 GB image memory and AOS Imaging Studio software, version 3.3.5.22 (AOS Technologies AG, Baden-Daettwil, Switzerland) at 800 x 600 pixel resolution, 21,986 μs exposure time, and 40 frames per second. Filming at walk beginning was triggered manually. Four LED floodlights (60 LEDs, 3.6 W) (BAHAG AG, Mannheim, Germany) mounted on poles were used to illuminate the stage. The floodlights were custom modified (Electronics Workshop, Animal Physiology Department, University of Cologne) to activate during exposure by a camera-provided internal frame trigger signal that produced a strobe output signal. Illumination intensity was adapted to exposure time.

ThF angle measurement

ThF angles were measured in five sequential steps during approximately straight walks on a cloth by frame-by-frame visual observation of the videos. The most protracted angles were defined as the time at which the leg being measured touched the substrate at the end of the swing. The most retracted angles were defined as the time at which the leg being measured lifted off the substrate at the end of stance. Stick insect bodies curve slightly during walking. Body orientation was therefore, for each leg, identified by one line running along the longitudinal body axis at the position where the leg being examined left the thorax. At the video resolution used in these experiments, the coxa is too small to be visualized. Any coxa-trochanterofemur joint angle could thus not be seen. Moreover, the fused trochanterofemur is slightly curved in some legs. Different degrees of pronation or supination of the ThC joint result in a more lateral or dorsal view of the trochanterofemur, and thus the appearance of the curve in some frames. The direction of the "coxa-trochanterofemur segment" was therefore identified with a line beginning where the leg left the thorax and extending as far as the trochanterofemur remained straight, depending on the leg, 20% to 50% of coxa-trochanterofemur total length. The angle between these two lines (the ThF angle) was measured using a Canvas (Deneba, Miami, FL, USA) built-in tool that measures the angle between two lines. Measurement accuracy was estimated to be 1°, and the angles measured by the Canvas built-in tool were therefore rounded to 1°.

QUANTIFICATION AND STATISTICAL ANALYSIS

"N" is animal number, "n" total number of data points per condition. All angles were rounded to 1° before further analysis. Significance levels: not significant (n.s.), $\alpha > 0.05$; *, $\alpha \leq 0.05$; **, $\alpha \leq 0.01$; ***, $\alpha \leq 0.001$. Plotting and all statistical tests in Table 1 were done in MATLAB (Version R2020a; The MathWorks, Natick, MA, USA). After plotting, figures were edited in CorelDraw X8 (Corel Corporation, Ottawa, Canada) and Canvas X. Data distribution normalities were tested using Anderson-Darling and Lilliefors tests in MATLAB. Because none of the angle data ranges exceeded 180°, all medians are linear medians, from which median absolute deviations were calculated, both in Kaleidagraph. Figure colors were chosen to maximize recognition by color vision impaired individuals.[63] The names of the chosen colors in Wong[63] were Black, Orange (RGB 230, 159, 0), Sky blue (RGB 86, 180, 233) and Reddish purple (RGB 204, 121, 167). We use here the terms black, orange, blue, and magenta.